Exploring the Highway Icing Risk: Considering the Dynamic Dependence of Icing-Inducing Factors

Qiang Liu
Harbin Institute of Technology
Aiping Tang (aipingtanghit@163.com)
Harbin Institute of Technology
Zhongyue Wang
Harbin Institute of Technology
Buyue Zhao
Beijing Jiaotong University

Research Article

Keywords: Dependence analysis, Exceeding probability, Hazard, Vulnerability, Transportation risk

Posted Date: April 22nd, 2021

DOI: https://doi.org/10.21203/rs.3.rs-445530/v1

Exploring the highway icing risk: Considering the dynamic dependence of icing-inducing factors

Qiang Liu [a], Aiping Tang [a, b *], Zhongyue Wang [a]，Buyue Zhao [c]

[a] *School of Civil Engineering, Harbin Institute of Technology, Harbin 150090, China*

[b] *Key Lab of Smart Prevention and Mitigation of Civil Engineering Disasters of the Ministry of Industry and Information Technology, Harbin Institute of Technology, Harbin150090, China*

[c] *School of Civil Engineering, Beijing Jiaotong University, Beijing 100044, China*

Abstract：In terms of the dynamic dependence between icing-inducing factors, this study is to explore the risk distribution of highways when icing events occur in the study area. A joint distribution considering the dynamic correlation of inducing factors was first constructed employing the Copula theory, which then yielded the possibility of icing events. Meanwhile, hazard zones and intensities of icing were proposed under different exceeding probabilities. After finishing the vulnerability analysis of highways, the risk matrix was used to conduct the icing risk for the highway, which was then applied to the construction of the risk zoning map. The results showed that there was an upper-tail dependence between extreme precipitation and temperature in the study area in winter, which could be well captured by the Gumbel Copula function. Indeed, the constructed joint distribution can express the possibility of icing under different intensities of precipitation and temperature. Besides, the highway with the tallest vulnerability in the study area was the Hegang-Yichun line. The case application showed that during March 2020, the traffic lines with a high icing risk were distributed around Fujin, Jiamusi, Hegang, and Qitaihe cities, and the Hegang section of the Hegang-Yichun line was at the highest icing risk. The low-risk lines were concentrated in the western part of the study area. This study is of great significance for the prevention and control of ice-snow disasters on the highway in cold regions.

Keywords: Dependence analysis; Exceeding probability; Hazard; Vulnerability; Transportation risk

1. Introduction

With the rapid changes in the climate today, the scale of natural disasters has shown an increasing trend in frequency and intensity (Zhan'e et al., 2011; Liu et al., 2016). Especially for meteorological disasters, temperature and precipitation display an extreme phenomenon in the context of global warming, which in turn has a significant impact on local infrastructure and life safety (Nourzad and Pradhan, 2015; Echavarren et al., 2019; Villalba Sanchis et al., 2020). Given the potential threats to the road due to the emergence of extreme weather in winter, carrying out the study on the icing risk of highways is of great significance to improve the safety of transportation in cold regions (Love et al., 2010; Andrey et al., 2017; Wang et al., 2020).

At present, many cases have carried out a series of studies on the risks caused by icing events on highways from the aspects of weather and road conditions, and pointed out that weather conditions are the main factors affecting traffic

* Corresponding author at: School of Civil Engineering, Harbin Institute of Technology. No.73 Huanghe Rd., Nangang Dist., Harbin 150090, China.
E-mail address: aipingtanghit@163.com

safety in winter (Usman et al., 2010; Gouda and El-Basyouny, 2020; Petrova, 2020). Further, physical simulation and indoor experimental research in terms of meteorological factors have always been hot spots in road icing (Shao and Lister, 1996; Andrey et al., 2017). Besides, taking the road surface temperature as the main parameter for early warning of road icing in winter and the safe operation and maintenance of the road has always been a focus of engineering applications. For example, Crevier (2001) regarded the road temperature as a controlling factor in the occurrence of icing events and then established a numerical simulation system with temperature as an indicator to predict road conditions (Crevier and Delage, 2001). Emerging artificial intelligence technologies have been applied to the analysis of winter road conditions, such as artificial neural networks, support vector machines, etc (Chang, 2005; Handler et al., 2020; Hegde and Rokseth, 2020). However, when the test sample has extreme values that exceed the range of the training sample, the predicted performance of the model will become very poor. Besides the above, data-driven statistical methods have been widely used in regional disasters, such as Poisson distribution, negative binomial regression distribution, Bayesian model, etc (Berrocal et al., 2010; Do, 2019). This type of method not only overcomes the difficulty of accurately simulating road icing using physical models and indoor tests but also does not have higher requirements on machine learning algorithms and data. R.Krsmanc (2013) selected traffic weather station data in three different environments, and concluded that the statistical model was better than the physical model in predicting road temperature through the comparison of regression statistical models and physical models. And with the new data collected, statistical models can be continuously improved, which can better provide forecasts for the evolution of road conditions in winter (Kršmanc et al., 2013). However, the literature shows that there are no many studies in the evaluation model that take into account the dependence between inducing factors, and fewer cases considering the dynamic dependence of inducing factors when the statistical model is used to analyze road icing (Zscheischler and Seneviratne, 2017).

Therefore, this study explores the dynamic dependence of the inducing factors of icing events based on data-driven statistical methods, especially the dependence under extreme weather, which was then applied to obtain the icing probability, thereby clarifying the icing hazard. After completing the vulnerability analysis of the regional highways, the risk matrix was used to carry out the icing risk assessment of the highway. Finally, a case of road icing in the study area was used to verify the applicability of the constructed method, to provide a reference for an emergency response to road icing in cold areas.

2. Study area environment and objects

The study area, Heilongjiang Province in Northeast China, lies between longitudes of 121°11' E and 135°05' E, and latitudes of 43°25' N and 53°33' N, which is in a cold temperate and a temperate continental monsoon zone, characterized by long cold winters. The study area is affected by the Mongolia-Siberian high pressure every year in winter, and the cold air brought by the high-pressure causes a large-scale cooling for the local area when it passes through the border. The average winter temperature is approximately -25℃. At the same time, the warm and humid airflow from the southern coastal area migrated northward driven by the pressure difference (Bihong et al., 2010; Fan and Tian, 2012). Eventually, the two encountered in the study area, resulting in different precipitation distribution over the study area (Fig. 1b).

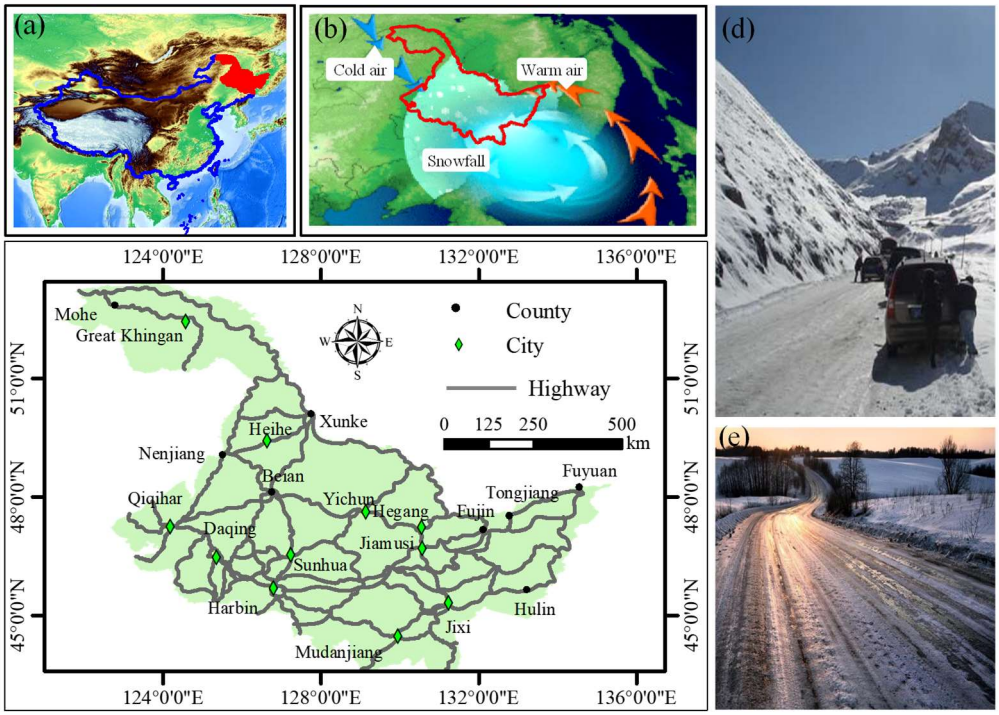

Fig. 1 Geographical location of the study area and its historical sites

Precipitation causes water or snow on the road surface, which provides material for road icing. When the temperature meets the icing conditions, the road surface with less precipitation will only maintain thin ice. As the precipitation increases, the road surface develops in the direction of ice coverage (Figs. 1e). Given the data availability, the average monthly precipitation (AMP) was used as an evaluation indicator for the material basis when road icing occurs. Pavement temperature is the controlling factor of road icing. Together with precipitation, it determines the development of road states, such as dryness, dampness, stagnant water and snow, slush, partial icing, and final ice cover (Crevier and Delage, 2001; Berrocal et al., 2010). The temperature of the road surface is determined by the temperature of the atmosphere. Here, the monthly average atmospheric temperature (AAT) was used as another indicator (Nantasai and Nassiri, 2017).

As the traffic lines are exposed to the natural environment, the operation of highways will be affected when an icing event occurs, such as vehicle speed reduction, road congestion, etc (Berdica, 2002; Somayeh et al., 2015). In this study, highways in different locations of the study area were used as disaster-bearing objects (Fig. 1c). For disaster-bearing bodies with different vulnerability characteristics, different risks will arise under the interference of icing with the same intensity (Birkmann, 2015). Compared with the less vulnerable disaster-bearing body, the more vulnerable hazard-bearing body is at a higher risk when involving the same hazard. Therefore, the vulnerability analysis of highways is an indispensable step in the study of road icing risk.

3. Methods

3.1 Hazard of the natural environment

Based on the disaster risk theory, the risk caused by the icing event to the highway in the study area can be divided into two parts, including the hazard and the vulnerability analysis (Beven et al., 2015). In this study, AMP and AAT

were regarded as the two main inducing factors for road icing. The joint distribution function of the inducing factors was established via the Copula theory, which is then used for the hazard analysis (Schölzel and P, 2008; Feng et al., 2017).

3.1.1 Construction of joint distribution

The joint distribution function is a probability function, which describes the probability that the dependent variable occurs under the combined action of multiple independent variables (Nelsen, 1997; Hotta, 2006; Hu, 2006). Since the probability of a disaster is determined by multiple inducing factors, the construction of a joint distribution function describing the probability of a disaster through inducing factors is the basis to accurately evaluate the hazard (Hochrainer-Stigler et al., 2018; Nguyen-Huy et al., 2019).

For the above purpose, Copula's theory states that any joint distribution function of n-variables can be decomposed into n corresponding unary edge distribution functions and a connecting function C describing the dynamic dependence between variables, namely the Copula function.

$$F(x_1, x_2, ..., x_n) = C\left[F(x_1), F(x_2), ..., F(x_n)\right] \quad (1)$$

where, $F(x_1, x_2, ...x_n)$ represents the joint distribution function of n variables, $F(x_i)$ is the edge distribution function of variable x_i, C stands for the Copula function, x_n is the nth independent variable.

Thus, the joint distribution function of the inducing factors of icing events under Copula theory can be constructed by using the marginal distribution functions of AMP and AAT, and a Copula function describing the dependence of inducing factors.

- **Marginal distribution function**

When it comes to the construction of the marginal distribution function, the weather data such as AMP and AAT from November to March of the following year were collected and counted, in the study area from 1999 to 2018. Because during this period, road icing and the resulting traffic accidents often occur. The data come from the Heilongjiang Provincial Bureau of Statistics and Heilongjiang Provincial Meteorological Information Center. Subsequently, empirical distribution functions of AMP and AAT were constructed by statistically performing sample data. When the statistical model converges, the optimal empirical distribution of the respective inducing factors was determined. Given the limitation of the sign of temperature on the search range of the edge distribution function, after obtaining the actual atmospheric temperature data, the absolute value of the temperature was taken as the sample data of the temperature distribution function for statistics.

- **Copula function**

At present, there are two ways to determine the Copula function. One is to generate the Copula function based on the function generator, and the other is to use the minimum squared Euclidean distance (MSED) to determine the optimal Copula function among many alternative Copula family functions (LI, 2000; Embrechts et al., 2002). Since the function generator needs to ensure that the marginal distribution functions of the inducing factors conform to the same distribution type when constructing, which is difficult to satisfy in general. Thus, the MSED method is widely

used in the measurement of the dependence of variables (Feng et al., 2017; Lazoglou and Anagnostopoulou, 2019). In this study, the MSED method was employed to determine the dependence between AMP and AAT. The candidate Copula functions were shown in Table 1. Generally, dependence described by these Copula clusters covers the characteristics of the dependence maintained between variables.

Table 1 The types of two-dimensional Copula family functions

Copula family	Type	Range of parameter: θ	Dependency characteristics	
			Symmetry	Tail dependence
Gaussian Copula	$C(u,v;\theta)=\int_{-\infty}^{\phi^{-1}(u)}\int_{-\infty}^{\phi^{-1}(v)}\frac{1}{2\pi\sqrt{1-\theta^2}}\exp(-\frac{x^2-2\theta xy+y^2}{2(1-\theta^2)})dxdy$	[-1, 1]	Y	N
T-Copula	$C(u,v;\theta)=\int_{-\infty}^{T^{-1}(u)}\int_{-\infty}^{T^{-1}(v)}\frac{1}{2\pi\sqrt{1-\theta^2}}\exp(1+\frac{x^2-2\theta xy+y^2}{v(1-\theta^2)})^{-(\frac{v+2}{2})}dxdy$	[-1, 1]	Y	Upper +Lower
Gumbel Copula	$C(u,v;\theta)=\exp(-(-\ln u)^{\theta}+(-\ln u)^{\theta})^{(1/\theta)})$	[1, ∞)	N	Upper
Frank Copula	$C(u,v;\theta)=-\frac{1}{\theta}\ln(1+\frac{(e^{-\theta u}-1)(e^{-\theta u}-1)}{e^{-\theta}-1})$	R	Y	N
Clayton Copula	$C(u,v;\theta)=\max((u^{-\theta}+v^{-\theta})^{-(1/\theta)},0)$	(0, ∞)	N	Lower

When using the MSED to determine the optimal Copula function, the Kendall rank correlation coefficient and the empirical Copula function of the inducing factors should be first calculated based on the sample data (Dianqing et al., 2012). Subsequently, parameters in different Copula functions were solved based on the Kendall rank correlation coefficient, further establishing the expression of different Copula functions for sample data. Finally, based on the MSED between different Copula functions and empirical Copula function, the Copula function with the minimum distance value was determined as the optimal Copula function to characterize the dependence between variables.

$$d^2(\hat{C}_n, C_k)=\sum_{i=1}^{n}|\hat{C}_n(u_i,v_i)\quad C(u_i,v_i)|^2=\sum_{i=1}^{n}|\hat{C}_n(F(x_i),G(y_i))\quad C(F(x_i),G(y_i))|^2 \tag{2}$$

where $d^2(\hat{C}_n, C_k)$ represents the square Euclidean distance between $\hat{C}_n$ and C_k, $\hat{C}_n$ depicts the empirical Copula, n is the number of samples, C_k depicts the candidate Copula function, u and v are the edge distribution function of variables x and y, respectively, x and y represent the AMP and AAT.

- **Joint distribution**

Copula theory shows that any n-ary joint distribution function can be decomposed into n corresponding unary distribution and a connection function describing the dependence between variables. In this study, the joint distribution function was jointly established by the marginal distribution of the inducing factors and the Copula function describing dependence between the AMP and AAT. The joint distribution function established based on the Copula theory not only can express the prediction of the probability of icing events by multiple factors but also the dependent changes of the inducing factors are embed in the joint distribution function.

3.1.2 Hazard analysis

Since the hazard is the product of abnormal changes in the natural environment, the hazard analysis and hazard zoning of icing events must be related to the spatial differentiation of the natural environment (Fotheringham et al., 2017; Kumar et al., 2017). In this study, the hazard analysis of the regional icing events was conducted based on the comprehensive zoning principle and the factor-dominant zoning principle of the territorial differentiation law.

In the principle of comprehensive zoning, different hazard zones were carried out based on the exceeding probability of icing events (Zscheischler and Seneviratne, 2017). Here, the exceeding probability of an icing event was defined as the occurrence rate (λ) where the hazard intensity s at different locations in the study area was greater than or equal to the given intensity s_a. That was the probability of $s \geq s_a$.

$$\lambda = P(s \geq s_a) = 1 - P(s \leq s_a) = 1 - H\left((x, y) \middle| x \leq x_a; y \leq y_a\right) \tag{3}$$

where λ denotes the exceeding probability, s_a is a given intensity of icing hazard, $P(s \geq s_a)$ represents the exceeding probability of the intensity that is greater than or equal to a given intensity value, and $H(x, y)$ is the joint distribution function of the indicators of inducing factors.

Since the hazard intensity of a disaster is determined by the different intensities of inducing factors, we can use the inducing factors with different intensities to measure the hazard intensity when the disaster occurs. According to the principle of factor dominance in this study, the inducing factors were solved based on the different exceeding probabilities, and then the intensity values of AMP and AAT under different hazard zones were obtained.

3.2 Vulnerability of disaster-bearing bodies

3.2.1 Vulnerability Indicators

According to disaster risk management theory, disaster-bearing bodies in the highway transportation system is the objects that disasters bring to bear on, and here it includes human, vehicle, road, etc, depicted by vulnerability (Yang et al., 2013). Currently, there is no consistent definition for vulnerability, depending on the research background (Jun-Qiang et al., 2017). Vulnerability of transportation generally is to evaluate the reduction of transportation performance under perturbation (Jenelius and Mattsson, 2015; Gonçalves and Ribeiro, 2020; Gu et al., 2020). At present, the analysis methods of transportation vulnerability are mainly based on the network topology, supply-demand, and based on the indicators (Bell et al., 2017; Gecchele et al., 2019; Shi et al., 2020). There is no optimal evaluation method, and different methods have different advantages and struggles. Here, the highway vulnerability was reflected from three aspects: sensitivity to disaster, resistance ability, and value exposure (Birkmann, 2015; Jafino et al., 2019).

Sensitivity reflects the characteristics of whether the highway is sensitive to the destructive power of a disaster, and is proportional to the vulnerability. Given the impact of icing events on highways, this study used the grades of the highway as an indicator to measure the sensitivity of the disaster-bearing body to icing events (Yang et al., 2013). In terms of resistance, in areas with better economic conditions, the repair and maintenance capabilities of highways after completion is more perfect, and the efficiency of emergency response during disasters and the recovery stage of

the road after the disaster is higher as well. That is, the socio-economic conditions can reflect a certain extent the robustness of the highways in the event of a disaster and the ability to restore to the initial state (Sugishita and Asakura, 2020). Here, GDP values of different regions in the study area were used to measure the local economic level. The nature of value exposure refers to the value or number of disaster-bearing bodies within the range of hazards. The exposure of the social value of highways is mainly reflected in the carrying capacity of the highway per unit length or area when the disaster occurs. There is no uniform standard for measuring social value. In this study, congestion information, in general, was employed to measure the social value of highways.

3.2.2 Vulnerability analysis

Based on the above three indicators, this study described the highway vulnerability as a function of damage sensitivity, resistance ability, and value exposure, which were applied to carry out the quantitative analysis of the highway vulnerability (Yang et al., 2013). Here, the vulnerability of the highway was measured by the vulnerability index, the greater the value, the greater the vulnerability:

$$\begin{cases} V = \dfrac{E^{*}S}{R} \\ V_s = \dfrac{V - V_{\min}}{V_{\max} - V_{\min}} \end{cases} \tag{4}$$

where E is the value exposure of the highway, S represents the damage sensitivity, R is the resistance ability, $V_{\max}$ and $V_{\min}$ represent the maximum and minimum values of the vulnerability in this study, respectively, V_s is the normalized vulnerability of highways.

3.3 Risk assessment and application

Risk assessment is the core link of disaster risk research (Peng et al., 2017; Wang et al., 2019). Currently, most scholars agree with the risk concept given by the Department of Humanitarian Affairs of the United Nations, that is, Risk = Hazard×Vulnerability (Birkmann, 2015; H and S, 2019). In this study, risk zoning of highways was carried out based on icing hazard zoning and highway vulnerability grade. In view of the icing risk encountered by the highways in the study area in the future, a risk matrix was employed here, and the highway icing risk was divided into five classes using the risk score, supplemented by five colors for representation (Table 2).

Table 2 Risk Matrix for classification

Scores of risk			Scores of Vulnerability grades				
			Grade I	Grade II	Grade III	Grade IV	Grade V
			1	2	3	4	5
Scores of hazard zones	Zone I	1	1	2	3	4	5
	Zone II	2	2	4	6	8	10
	Zone III	3	3	6	9	12	15
	Zone VI	4	4	8	12	16	20
	Zone V	5	5	10	15	20	25

where the red represents an extremely high risk, with the score of 1-2; Orange represents a high risk, with the score of 3-5; Yellow represents a medium risk, with the score of 6-10; Green represents a low risk, with the score of 12-16; Blue represents an extremely low risk, with the score of 20-25.

Around March 5, 12, 18, and 26, 2020, four heavy snowfalls occurred in Heilongjiang Province, causing the continuous closure of many highways in the study area, including the lines of Harbin-Tongjiang, Hegang-Jiamusi, and Hegang-Yichun over the study area, which seriously affected the operation of the local transportation. Taking the AMP and AAT in March 2020 as an example, the hazard analysis of icing disasters was carried out, and on this basis, road icing risk assessment was carried out as well. In this case, the joint distribution function of inducing factors was first used to calculate the exceeding probability of icing events in the study area during this period. Subsequently, in contrast to the hazard of icing events, the exceeding probability was related to the corresponding hazard zone. The higher the zone level is, the greater the hazard intensity of the icing. Consequently, the corresponding road risk was determined based on the risk matrix.

4 Results

4.1 Hazard results

4.1.1 Marginal distribution

The marginal distribution function is the basis for constructing a joint distribution function. Based on the statistics of the frequency of precipitation and temperature, the edge distribution functions of the inducing factors with the optimal accuracy under the convergence condition are determined (Fig. 2). The optimal distribution of precipitation is a first-order exponential decay function. The model determination coefficient (R^2) after the parameter test is 0.9951, which indicates that the independent variable x can explain 99.51% of the change in F(x) through the mapping relationship of the optimal model.

$$u = F(x) = -1.07 * e^{\left(\frac{-x}{9.74}\right)} + 1.04 \quad (5)$$

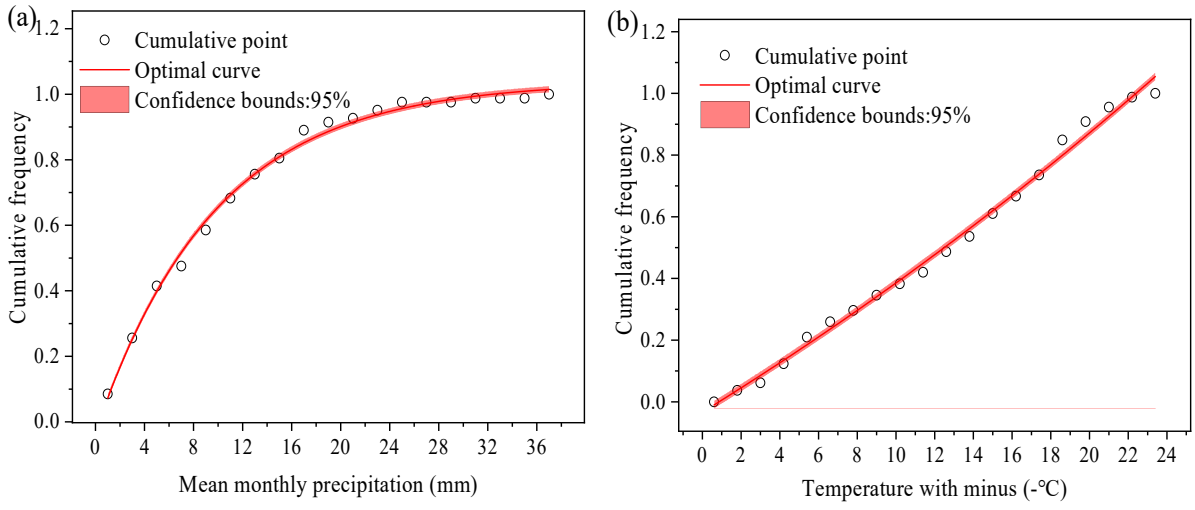

Fig. 2 Marginal distribution function of inducing factors, (a)AMP, (b) AAT

The possibility of different intensities of AAT in the study area is shown in Fig. 2b. The determination coefficient (R^2) of the optimal model is 0.9884, which indicates that for the change of the dependent variable G(y), the independent variable y can obtain a 98.84% response through the functional relationship of the optimal model.

$$v = G(y) = 2.59 * e^{\left(\frac{y}{66.71}\right)} - 2.62 \quad (6)$$

4.1.2 Joint distribution

The Euclidean distance between each candidate Copula function and the empirical Copula function is shown in Table 3. The distance between Gaussian Copula and empirical Copula is 1.2434; the distance between T-Copula and empirical Copula is 0.9455; the distance between Gumbel Copula and empirical Copula is 0.0521; the distance between Frank Copula and empirical Copula is 0.0892, and the distance between Clayton Copula and empirical Copula is 0.1207.

Table 3 Euclidean distance values for different candidate functions

Copula family	Gaussian Copula	T-Copula	Gumbel Copula	Frank Copula	Clayton Copula
Euclidean distance	1.2434	0.9455	0.0521	0.0892	0.1207

Compared with the other four types of Copula, the Euclidean distance between Gumbel Copula and the empirical Copula is the smallest, which can better characterize the dependence between AMP and AAT in the study area (Fig. 3). Thus, the depiction of the dependence of inducing factors can be expressed better by the Gumbel Copula.

$$C(u,v) = \exp(-(-\ln u)^{2.88} + (-\ln u)^{2.88})^{0.35}) \quad (7)$$

where C(u,v) is the Gumbel Copula function, u and v represent the marginal distribution functions of the two factors of AMP and AAT, respectively.

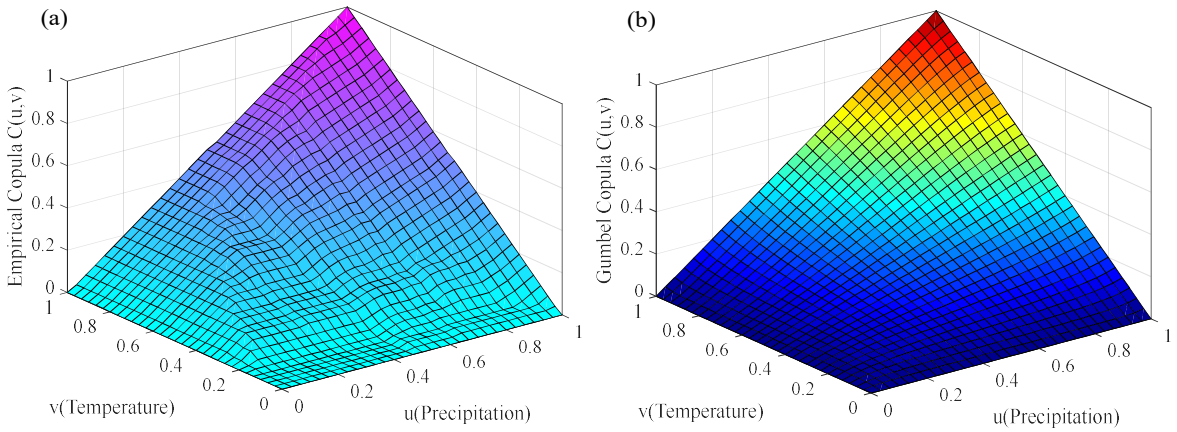

Fig. 3 Dependence of inducing factors, (a) Empirical Copula, (b) Gumbel Copula

The Gumbel density function was used here to visually describe the occurrence possibility of icing-inducing factors in the study area, and further demonstrate the dependency changes (Fig. 4a). Results show that there is an upper tail dependence between the average monthly precipitation and the average atmospheric temperature. After determining the marginal distribution and Copula function, the joint distribution based on Copula theory is as follows:

$$\begin{cases} H(x,y) = C(u,v) = e^{(-(-\ln u)^{2.88}+(-\ln v)^{2.88})^{0.35}} \\ u = F(x) = -1.07 * e^{\left(\frac{-x}{9.74}\right)} + 1.04 \\ v = G(y) = 2.59 * e^{\left(\frac{y}{66.71}\right)} - 2.62 \end{cases} \quad (8)$$

where $H(x, y)$ represents the joint distribution function of icing-inducing factors; u, v represents the edge distribution function of AMP, AAT, respectively; C represents the Copula function; x, y are the mean monthly snowfall, atmosphere temperature, respectively. Indeed, the spatial surface of the joint distribution function under different temperatures and precipitation is shown in Fig. 4, which contains the changing trends of Fig. 2 (a) and (b) together, and can simultaneously depict the probability of precipitation and temperature.

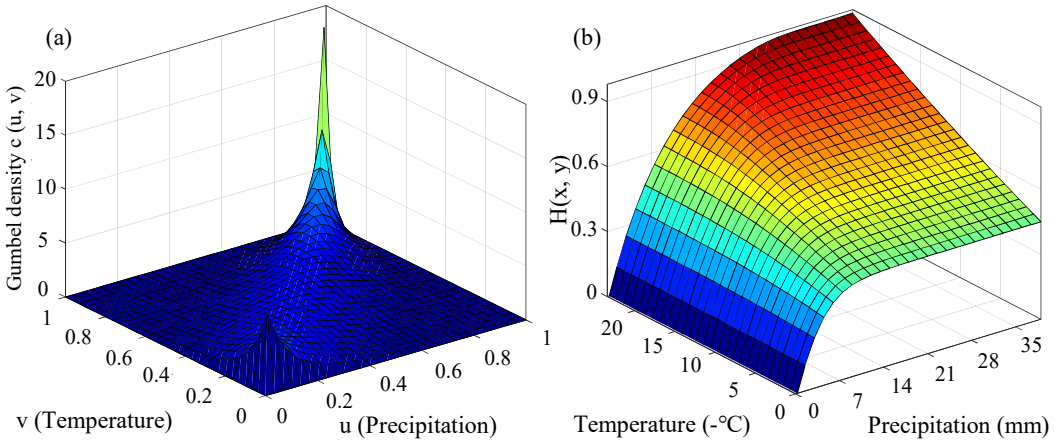

Fig. 4 Probability of inducing factors (a) Dependency change; (b) Joint distribution

4.1.3 Hazard zone

Conducting hazard zoning is conducive to realizing the zoning management and hierarchical control for disasters. Here, in the principle of comprehensiveness, based on the joint distribution function of inducting factors, the hazard of icing hazards is divided into five zones according to the exceeding probability (Fig. 5a). Hazard zones are from high to low: Zone I, Zone II, Zone III, Zone IV, and V.

Table 4 Hazard zoning of icing events under different exceeding probability

Hazard zoning		Zone I	Zone II	Zone III	Zone IV	ZoneV
Exceeding probability		<0.13	0.13~ 0.29	0.29~ 0.51	0.51~0.76	>0.76
Possibility		Very low	Low	Medium	High	Very high
Intensity		Very high	High	Medium	Low	Very low
Intensity level	Precipitation(mm)	>17.92	11.84~17.92	6.87~11.84	2.93~6.87	<2.93
	Temperature (℃)	<-19.96	-19.96~-16.92	-16.92~-12.38	-12.38~-6.67	>-6.67

Based on the above zoning, the occurrence possibility, hazard zone, and intensity are linked together through the exceeding probability, which intuitively presents the relationship in Fig. 5a. From the perspective of the corresponding relationship, the lower the exceeding probability of a disaster, the higher the hazard intensity and the

hazard zone when a disaster occurs in the future, which also shows that the intensity and frequency of icing disaster are negatively correlated.

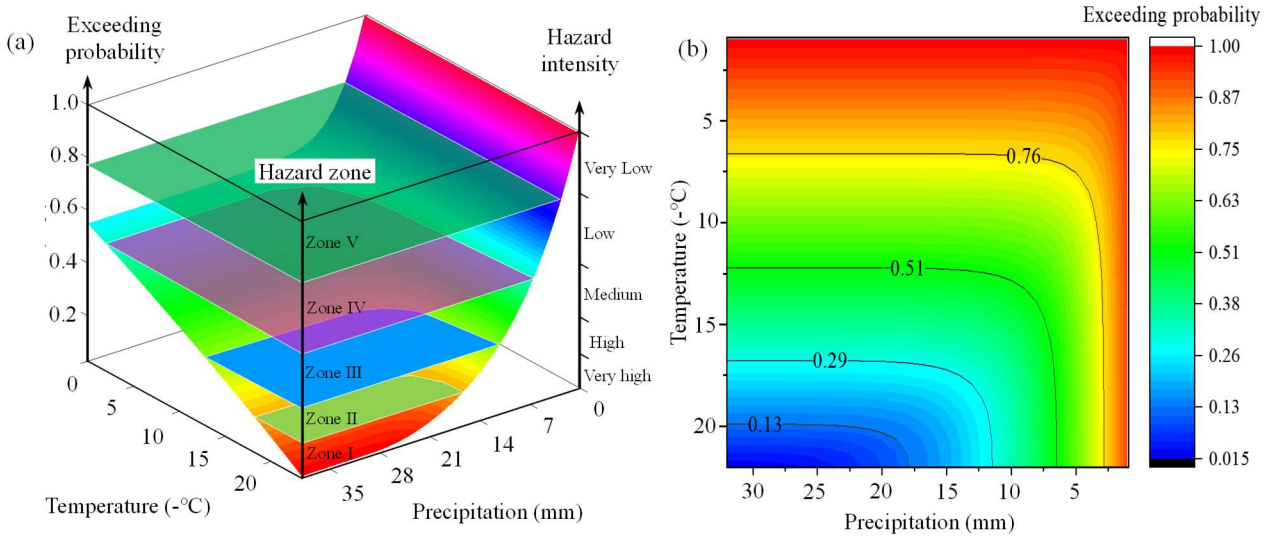

Fig. 5 The hazard of icing disaster, (a) Hazard zone, (b) Hazard level

The respective hazard levels of AMP and AAT under different hazard zones are solved based on the exceeding probability, according to the principle of factor dominance (Table 4). This phenomenon can be presented intuitively from the contour map of the exceeding probability (Fig. 5b). The application of the principle of factor dominance can achieve the rapid assessment of icing disasters so that timely material allocation and emergency treatment can be carried out for post-disaster rescue.

4.2 Vulnerability Results

4.2.1 Vulnerability indicators

In view of the impact of icing events on highways, the sensitivity distribution of disaster-bearing bodies is measured by highway grades (Fig. 6a). The higher the highway grade is, the lower the sensitivity of the road itself to icing disaster. Considering the availability of data, the GDP value is used to reflect the economic conditions for a region to a certain extent. GDP values of different regions in the study area are used as an indicator to measure the local economic level (Fig. 6b). It is inversely proportional to vulnerability. Vulnerability is proportional to the value exposure of the disaster-bearing bodies. The more congested the road, the greater the value exposure of the highway when it is subjected to an icing event, and the greater the ultimate vulnerability. The value exposure of highways in the study area during service is shown in Fig. 6c.

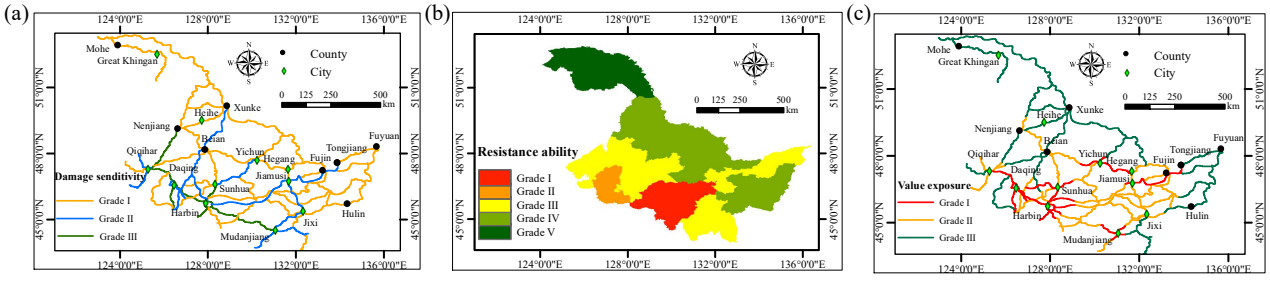

Fig. 6 Vulnerability indicators, (a) Damage sensitivity, (b) Economic conditions, (c) Value exposure

4.2.2 Vulnerability distribution

Vulnerability in this study is divided into five grades according to the natural breakpoint method in the geographical information system (GIS), which can minimize the internal data of each grade and maximize the differences between grades. Vulnerability grades from high to low are grade I, grade II, grade III, grade IV, and V. The higher the grade, the more vulnerable it is when suffering from disasters (Table 5).

Table 5 vulnerability grades of highways

Vulnerability grades	Grade I	Grade II	Grade III	Grade IV	Grade V
Vulnerability Index	>0.86	0.73~0.86	0.51~0.73	0.35~0.51	<0.35

On the basis of grade division, GIS technology was applied to construct the vulnerability zoning map of highways to explore the spatial distribution of the highway vulnerability (Fig. 7). The analysis shows that the Hegang-Yichun line has the highest vulnerability in the study area. The following are the lines of Mohe-Great Khingan, Mohe-Xunke, Suihua-Daqing, Neijaing-Beian-Suihua, and near the Qitaihe, Fujin cities. The transportation line with the lowest vulnerability is the Nenjiang-Qiqihar section.

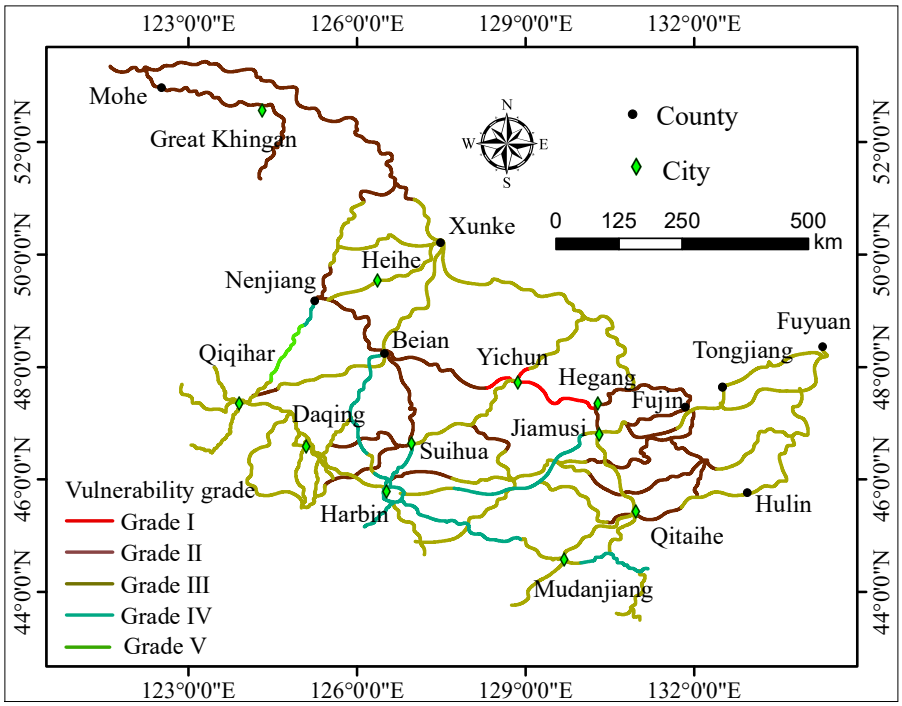

Fig. 7 Vulnerability distribution of highways

4.3 Risk application

For the case application in this study, the icing hazard in the study area during this period determined by the exceeding probability mainly involves three zones (Table 6). As GIS has an outperformed spatial analysis ability, it is used here for the icing-hazard zoning, which can improve the accuracy of hazard assessment (Toma-Danila et al., 2020). Moreover, under the condition that the highway vulnerability remains unchanged, the spatial overlap about

the hazard in the case with the highway vulnerability is realized (Fig. 8a).

Table 6 Highway risk in case application

Highways risk			Vulnerability grades				
			Grade I	Grade II	Grade III	Grade IV	Grade V
Hazard zones	Zone II: Exceeding probability	0.13-0.29	2	4	6	8	10
	Zone III: Exceeding probability	0.29-0.51	3	6	9	12	15
	Zone IV: Exceeding probability	0.51-0.76	4	8	12	16	20

Regarding the impact of icing events on highways, after constructing the hazard distribution map of icing events, the concept of the risk matrix is applied to GIS, and finally output results in the form of a risk zoning map to visually display highways risk during this period (Fig. 8b). Risk results show that in the case analysis, the traffic line with the highest risk class is the Hegang section of the Hegang-Yichun line. Meanwhile, highways surrounding Fujin, Qitaihe, and Jiamusi also have a greater impact, which is consistent in the road condition information released by the Provincial Traffic Information Center. Meanwhile, transportation lines with low-risk classes are generally located at the west of the study area, mainly distributed in Qiqihar, Daqing, and Xunke areas.

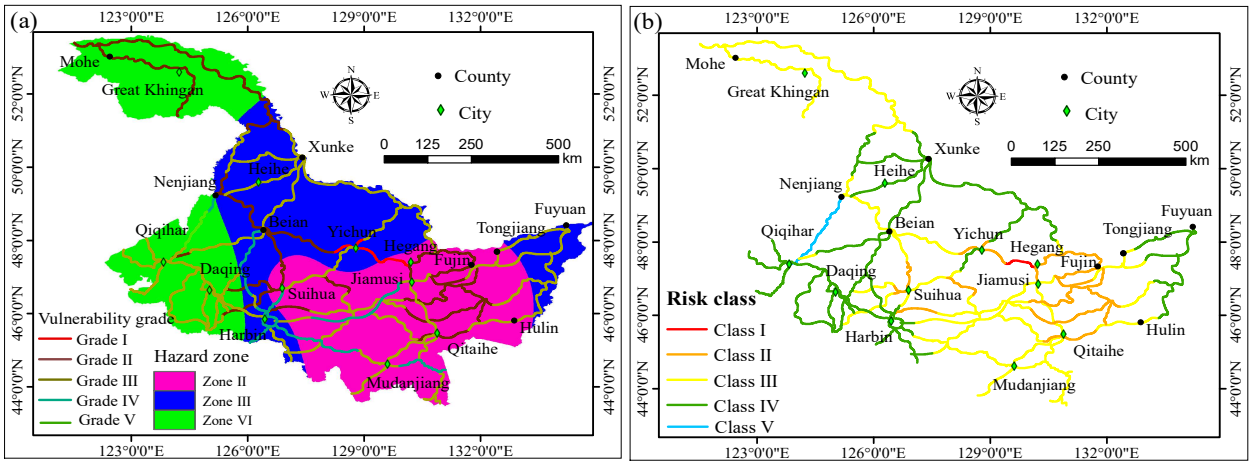

Fig. 8 Highway icing analysis, (a) Spatial overlap of hazard and vulnerability, (b) Highway risk distribution

5 Discussion

The joint distribution of ice-inducing factors established based on the Copula theory takes into account the dynamic dependence of the inducing factors. The results show that there is an upper-tail dependency between monthly precipitation and atmospheric temperature (Lazoglou and Anagnostopoulou, 2018). Moreover, when extreme weather occurs, the interdependence between AMP and AAT will gradually increase. That is, in winter, higher precipitation is generally accompanied by lower temperature, and the possibility of low temperature inducing precipitation is great as well. Typically, the Gumbel Copula can better capture this information and describe it (Fig. 4a).

The risk of highway icing is related to the icing-inducing factors of different regions in the study area and the distribution of highway vulnerability. Case studies have shown that as the highway vulnerability is relatively stable

over a period of time, the icing risk encountered by highways is directly related to the possibility of icing events each year, which further depends on the inducing factors of icing. In other words, we can directly assess the icing risk of the highway in the future based on the forecast of temperature and precipitation in the aspect of the weather forecast. This can not only complete the post-disaster deicing and relief of icing disasters but also realize the rapid assessment and early warning of icing risks before the disaster.

It should be pointed out that the occurrence of icing disasters is not only related to precipitation and temperature but also related to the wind, not considered in this study, including wind speed and direction (Somayeh et al., 2015). Moreover, the quantitative analysis of disaster-bearing bodies needs to be improved in the future as well. It is not only the sensitivity, resistance, and value exposure, but also the topology structure of the road network. How to embed the topological vulnerability of highways into the highway vulnerability needs to be explored in the future (Faturechi and Miller-Hooks, 2015; Mattsson and Jenelius, 2015).

6 Conclusions

This study explored the possibility of icing disasters through the inducing factors of icing events, and then completed the risk assessment of icing disasters on highways in the study area. The results showed that:

(1) Optimal Copula determined based on the Euclidean distance showed a high upper tail dependence between precipitation and temperature during icing, which could be captured by Gumbel Copula. This phenomenon showed that there is a high dependence on the occurrence of low temperature and strong precipitation in extreme weather. Moreover, changeable dependence could be embedded in the joint distribution function of inducing factors and further used in the prediction of icing events.

(2) From the perspective of the law of regional differentiation, this study put forward the point of view that disaster hazard zoning should be combined with the differentiation of the natural environment, which provided a basis for hazard zoning. Meanwhile, taking the exceeding probability as the starting point, hazard zoning of the icing was conducted, and the critical values of the hazard intensity under different zones were determined, which provided a reference for the rapid assessment of icing disasters. In addition, the hazard assessment of icing disasters based on exceeding probability connected the occurrence probability of icing events, the hazard zone, and intensity, and formed the hazard assessment theory of icing disasters.

(3) The highway vulnerability constructed based on damage sensitivity, resistance, and value exposure indicated that the highway with the highest vulnerability grade in the study area was the Hegang-Yichun line. The case application showed that the line with the highest risk of road icing in the study area was the Hegang section of the Hegang-Yichun line. Meantime, the highways around Fujin, Qitaihe, and Jiamusi also had a greater impact, which is in line with the road information released by the provincial traffic center indicating the applicability of the method in this study.

It needs to be pointed out that analysis of the highway vulnerability still needs to be improved in this study. Integrating structural vulnerability and functional vulnerability of highways to construct a quantitative vulnerability evaluation method is an issue that needs to be solved in the future.

Acknowledgments

This research was supported and funded by the National Key Research and Development Program of China (2016YFE0202400 and 2018YFC0809605), aiming to study the interaction between natural disasters and engineering infrastructure in cold regions. The authors were grateful for this support and would also like to thank the professors for providing the dates used in this study.

Conflicts of interest

The authors declare that there is no conflict of interest. Some or all data, models, or codes generated or used during the study are available from the corresponding author by request.

References

Andrey, J., Matthews, L.,Picketts, I., 2017. Planning for Winter Road Maintenance in the Context of Climate Change. Weather, Climate, and Society 9, 521-532.

Bell, M.G.H., Kurauchi, F., Perera, S.,Wong, W., 2017. Investigating transport network vulnerability by capacity weighted spectral analysis. Transport. Res. B-Meth. 99, 251-266.

Berdica, K., 2002. An introduction to road vulnerability: what has been done, is done and should be done. Transport Policy 9, 117-127.

Berrocal, V.J., Raftery, A.E., Gneiting, T.,Steed, R.C., 2010. Probabilistic weather forecasting for winter road maintenance. Journal of the American Statistical Association 105.

Beven, K.J., Aspinall, W.P., Bates, P.D., Borgomeo, E., Goda, K., Hall, J.W., Page, T., Phillips, J.C., Rougier, J.T., Simpson, M., Stephenson, D.B., Smith, P.J., Wagener, T.,Watson, M., 2015. Epistemic uncertainties and natural hazard risk assessment – Part 1: A review of the issues. Natural Hazards and Earth System Sciences Discussions 3, 7333-7377.

Bihong, X., Changyuan, S., Jing, Z.,Kairong, Z., 2010. Analysis on the Heavy Snowstorm Process in Northeast China during March 3－5 in 2007. Meteorological and Environmental Research 1, 15-19.

Birkmann, J., 2015. Assessing the risk of loss and damage，exposure, vulnerability and risk to climate-related hazards for different country classifications. International Journal of Global Warming 8, 191-212.

Chang, L.-Y., 2005. Analysis of freeway accident frequencies: Negative binomial regression versus artificial neural network. Safety Science 43, 541-557.

Crevier, L.P.,Delage, Y., 2001. METRo: a new model for road-condition forecasting in Canada. Journal of Applied Meteorology 40, 2026-2037.

Dianqing, L., Xiaosong, T., Chuangbing, Z.,Kok-Kwang, P., 2012. Uncertainty analysis of correlated non-normal geotechnical parameters using Gaussian copula. Science China Technological Sciences 55, 3081-3089.

Do, M., 2019. Estimation of Road Pavements Life Expectancy via Bayesian Markov Mixture Hazard Model. 21, 57-67.

Echavarren, J.M., Balžekienė, A.,Telešienė, A., 2019. Multilevel analysis of climate change risk perception in Europe: Natural hazards, political contexts and mediating individual effects. Safety Science 120.

Embrechts, P., McNeil, A.J.,Straumann, D. 2002 Correlation and Dependence in Risk Management: Properties and Pitfalls, Risk Management, pp. 176-223.

Fan, K.,Tian, B., 2012. Prediction of wintertime heavy snow activity in Northeast China. Chinese Science Bulletin 58, 1420-1426.

Faturechi, R.,Miller-Hooks, E., 2015. Measuring the Performance of Transportation Infrastructure Systems in Disasters: A Comprehensive Review. J. Infrastruct. Syst. 21.

Feng, J., Li, N., Zhang, Z.,Chen, X., 2017. How to apply the dependence structure analysis to extreme temperature and precipitation for disaster risk assessment. Theoretical and Applied Climatology 133, 297-305.

Fotheringham, A.S., Yang, W.,Kang, W., 2017. Multiscale Geographically Weighted Regression (MGWR). Ann. Am. Assoc. Geogr. 107, 1247-1265.

Gecchele, G., Ceccato, R.,Gastaldi, M., 2019. Road Network Vulnerability Analysis: Case Study Considering Travel Demand and Accessibility Changes. J. Transp. Eng. A-Syst. 145.

Gonçalves, L.A.P.J.,Ribeiro, P.J.G., 2020. Resilience of urban transportation systems. Concept, characteristics, and methods. J. Transp. Geogr. 85.

Gouda, M.,El-Basyouny, K., 2020. Before-and-after empirical bayes evaluation of achieving bare pavement using anti-icing on urban roads. Transportation Research Record 2674, 92-101.

Gu, Y., Fu, X., Liu, Z., Xu, X.,Chen, A., 2020. Performance of transportation network under perturbations: Reliability, vulnerability, and resilience. Transport. Res. E-Log. 133.

H, C.,S, C., 2019. Risk-matrix analysis on disasters and accidents to establish investment directions of budgeting for disasters and safety management. Journal of The Korean Society of Hazard Mitigation 19, 165-179.

Handler, S.L., Reeves, H.D.,McGovern, A., 2020. Development of a Probabilistic Subfreezing Road Temperature Nowcast and Forecast Using Machine Learning. Weather and Forecasting 35, 1845-1863.

Hegde, J.,Rokseth, B., 2020. Applications of machine learning methods for engineering risk assessment – A review. Safety Science 122.

Hochrainer-Stigler, S., Pflug, G., Dieckmann, U., Rovenskaya, E., Thurner, S., Poledna, S., Boza, G., Linnerooth-Bayer, J.,Brännström, Å., 2018. Integrating Systemic Risk and Risk Analysis Using Copulas. International Journal of Disaster Risk Science 9, 561-567.

Hotta, L.K., 2006. Using conditional Copula to estimate value at risk. Journal of Data Science 4, 93-115.

Hu, L., 2006. Dependence patterns across financial markets: a mixed copula approach. Applied Financial Economics 16, 717-729.

Jafino, B.A., Kwakkel, J.,Verbraeck, A., 2019. Transport network criticality metrics: a comparative analysis and a guideline for selection. Transport Rev. 40, 241-264.

Jenelius, E.,Mattsson, L.-G., 2015. Road network vulnerability analysis: Conceptualization, implementation and application. Computers, Environment and Urban Systems 49, 136-147.

Jun-Qiang, L., Long-Hai, Y., Liu, W.Y.,Zhao, L., 2017. Measuring Road Network Vulnerability with Sensitivity Analysis. PLoS One 12, e0170292.

Kršmanc, R., Slak, A.Š.,Demšar, J., 2013. Statistical approach for forecasting road surface temperature. Meteorological Applications 20, 439-446.

Kumar, S., Srivastava, P.K.,Snehmani, 2017. Geospatial Modelling and Mapping of Snow Avalanche Susceptibility. J. Indian Soc. Remote 46, 109-119.

Lazoglou, G.,Anagnostopoulou, C., 2018. Joint distribution of temperature and precipitation in the Mediterranean, using the Copula method. Theoretical and Applied Climatology 135, 1399-1411.

Lazoglou, G.,Anagnostopoulou, C., 2019. Joint distribution of temperature and precipitation in the Mediterranean, using the Copula method. Springer Vienna 135.

LI, D.X., 2000. On Default Correlation，A Copula Function Approach. The Journal of Fixed Income 09, 43-54.

Liu, C., Kershaw, T., Eames, M.E.,Coley, D.A., 2016. Future probabilistic hot summer years for overheating risk assessments. Building and Environment 105, 56-68.

Love, G., Soares, A.,Püempel, H., 2010. Climate Change, Climate Variability and Transportation. Procedia Environmental Sciences 1, 130-145.

Mattsson, L.-G.,Jenelius, E., 2015. Vulnerability and resilience of transport systems – A discussion of recent research. Transportation Research Part A 81, 16-34.

Nantasai, B.,Nassiri, S., 2017. Winter temperature prediction for near-surface depth of pervious concrete pavement. International Journal of Pavement Engineering 20, 820-829.

Nelsen, R.B., 1997. Dependence and order in families of Archimedean Copulas. Journal of Multivariate Analysis 60, 111-122.

Nguyen-Huy, T., Deo, R.C., Mushtaq, S., Kath, J.,Khan, S., 2019. Copula statistical models for analyzing stochastic dependencies of systemic drought risk and potential adaptation strategies. Stochastic Environmental Research and Risk Assessment 33, 779-799.

Nourzad, S.H.H.,Pradhan, A., 2015. Vulnerability of infrastructure systems: macroscopic analysis of critical disruptions on road networks. Journal of Infrastructure Systems.

Peng, C., Regmi, A.D., Qiang, Z., Yu, L., Xiaoqing, C.,Deqiang, C. 2017 Natural Hazards and Disaster Risk in One Belt One Road Corridors, Advancing Culture of Living with Landslides, pp. 1155-1164.

Petrova, E., 2020. Natural hazard impacts on transport infrastructure in Russia. Natural Hazards and Earth System Sciences 20, 1983-1969.

Schölzel, C.,P, F., 2008. Multivariate non-normally distributed random variables in climate research – introduction to the copula approach. Nonlinear Processes in Geophysics 15, 761-772.

Shao, J.,Lister, P.J., 1996. An Automated Nowcasting Model of Road Surface Temperature and State for Winter Road Maintenance. Journal of Applied Meteorology 35, 1352-1361.

Shi, Y., Blainey, S., Sun, C.,Jing, P., 2020. A literature review on accessibility using bibliometric analysis techniques. J. Transp. Geogr. 87.

Somayeh, N., Alireza, B.,Sahar, S., 2015. Survey of Practice and Literature Review on Municipal Road Winter Maintenance in Canada. Journal of Cold Regions Engineering 29, 1-18.

Sugishita, K.,Asakura, Y., 2020. Vulnerability studies in the fields of transportation and complex networks: a citation network analysis. J. Public Transport.

Toma-Danila, D., Armas, I.,Tiganescu, A., 2020. Network-risk: an open GIS toolbox for estimating the implications of transportation network damage due to natural hazards, tested for Bucharest, Romania. Natural Hazards and Earth System Sciences 20, 1421-1439.

Usman, T., Fu, L.,Miranda-Moreno, L.F., 2010. Quantifying safety benefit of winter road maintenance: accident frequency modeling. Accid Anal Prev 42, 1878-1887.

Villalba Sanchis, I., Insa Franco, R., Martínez Fernández, P., Salvador Zuriaga, P.,Font Torres, J.B., 2020. Risk of increasing temperature due to climate change on high-speed rail network in Spain. Transport. Res. D-Tr. E. 82.

Wang, J., Bu, K., Yang, F., Yuan, Y., Wang, Y., Han, X.,Wei, H., 2019. Disaster Risk Reduction Knowledge Service: A Paradigm Shift from Disaster Data Towards Knowledge Services. Pure Appl. Geophys. 177, 135-148.

Wang, T., Qu, Z., Yang, Z., Nichol, T., Clarke, G.,Ge, Y.-E., 2020. Climate change research on transportation systems: Climate risks, adaptation and planning. Transportation Research Part D: Transport and Environment 88.

Yang, J., Sun, H., Wang, L., Li, L.,Wu, B., 2013. Vulnerability evaluation of the highway transportation system against meteorological disasters. Procedia - Social and Behavioral Sciences 96.

Zhan'e, Y., Jie, Y., Shiyuan, X.,Jiahong, W., 2011. Community-based scenario modelling and disaster risk assessment of urban rainstorm waterlogging. Journal of Geographical Sciences 21, 274-284.

Zscheischler, J.,Seneviratne, S.I., 2017. Dependence of drivers affects risks associated with compound events. Science Advances, 3, e1700263.

Figures

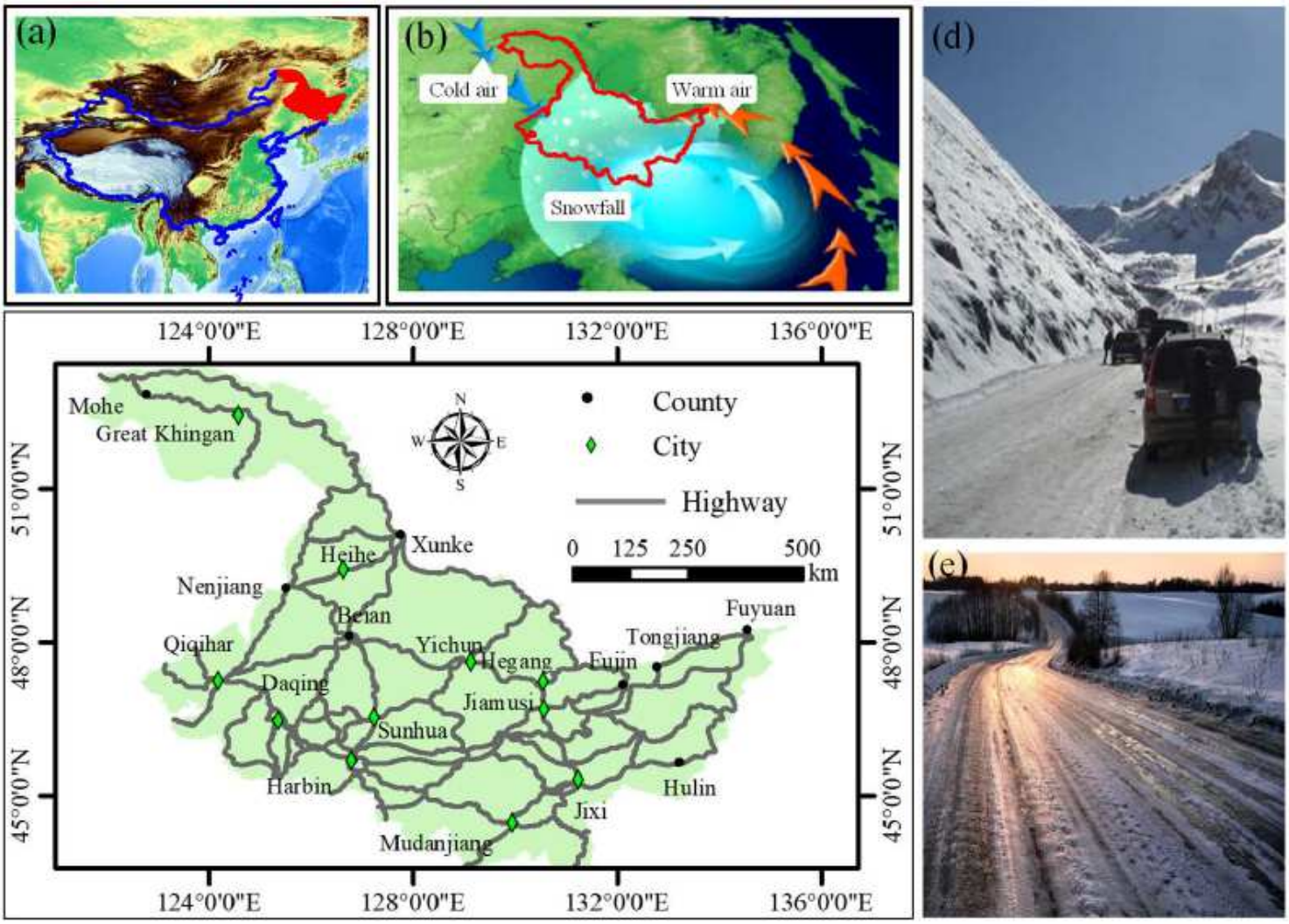

Figure 1

Geographical location of the study area and its historical sites Note: The designations employed and the presentation of the material on this map do not imply the expression of any opinion whatsoever on the part of Research Square concerning the legal status of any country, territory, city or area or of its authorities, or concerning the delimitation of its frontiers or boundaries. This map has been provided by the authors.

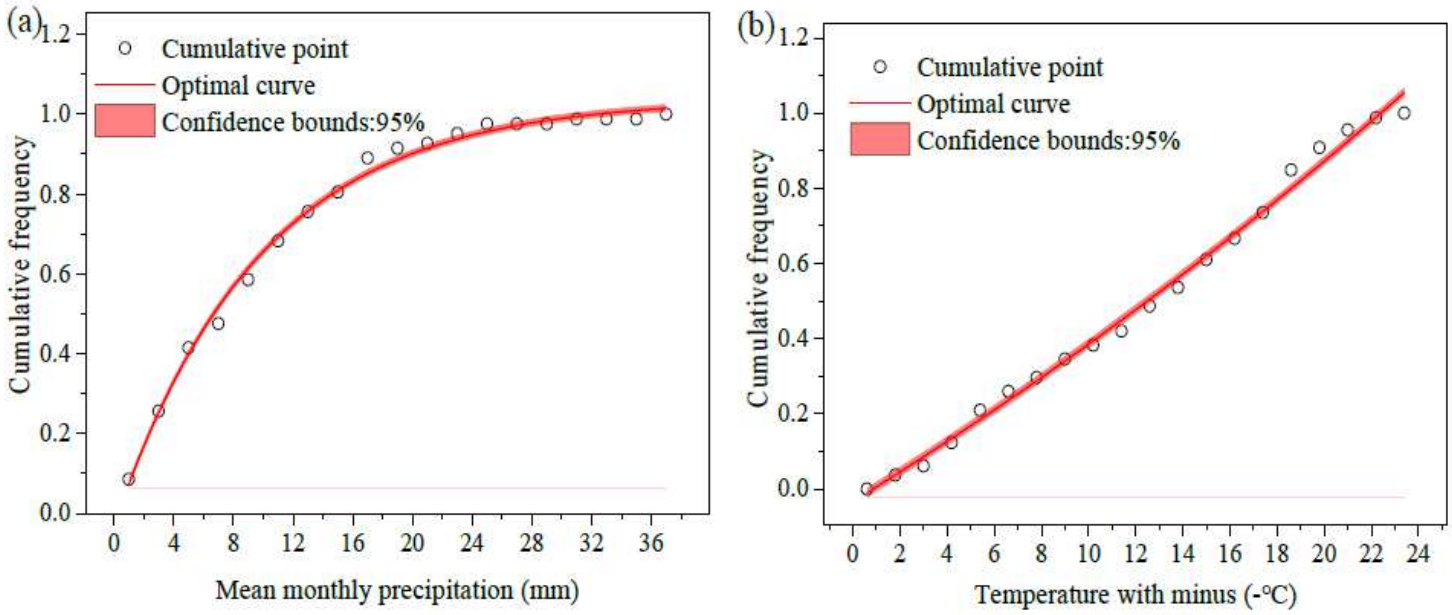

Figure 2

Marginal distribution function of inducing factors, (a)AMP, (b) AAT

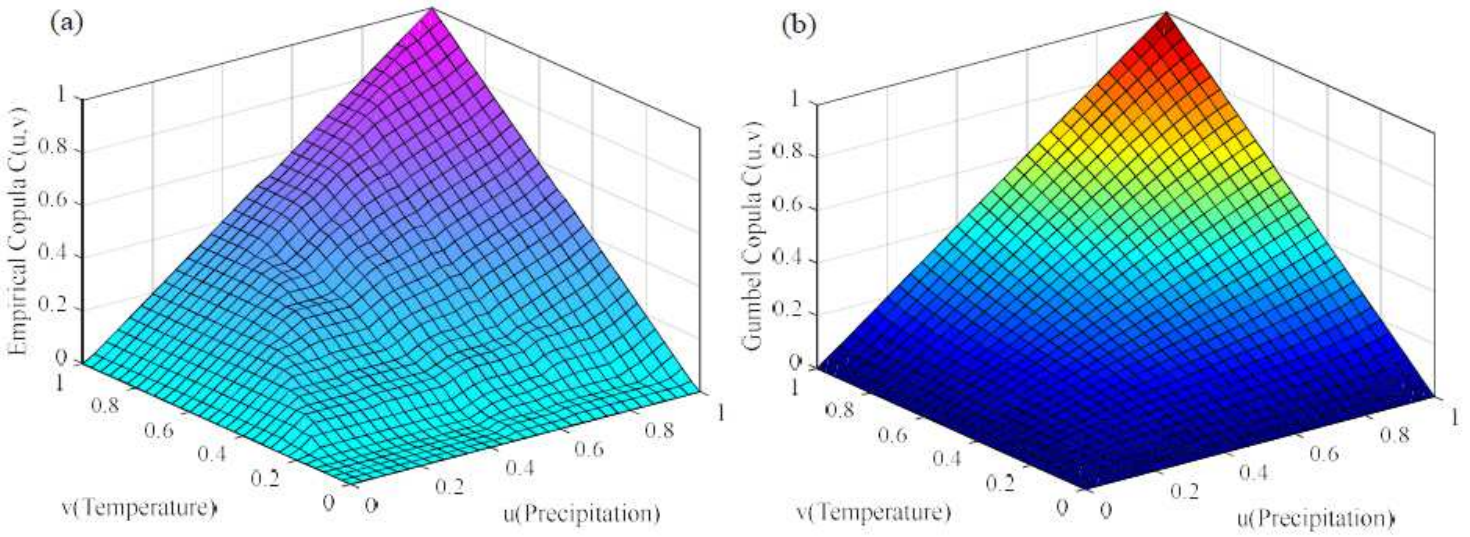

Figure 3

Dependence of inducing factors, (a) Empirical Copula, (b) Gumbel Copula

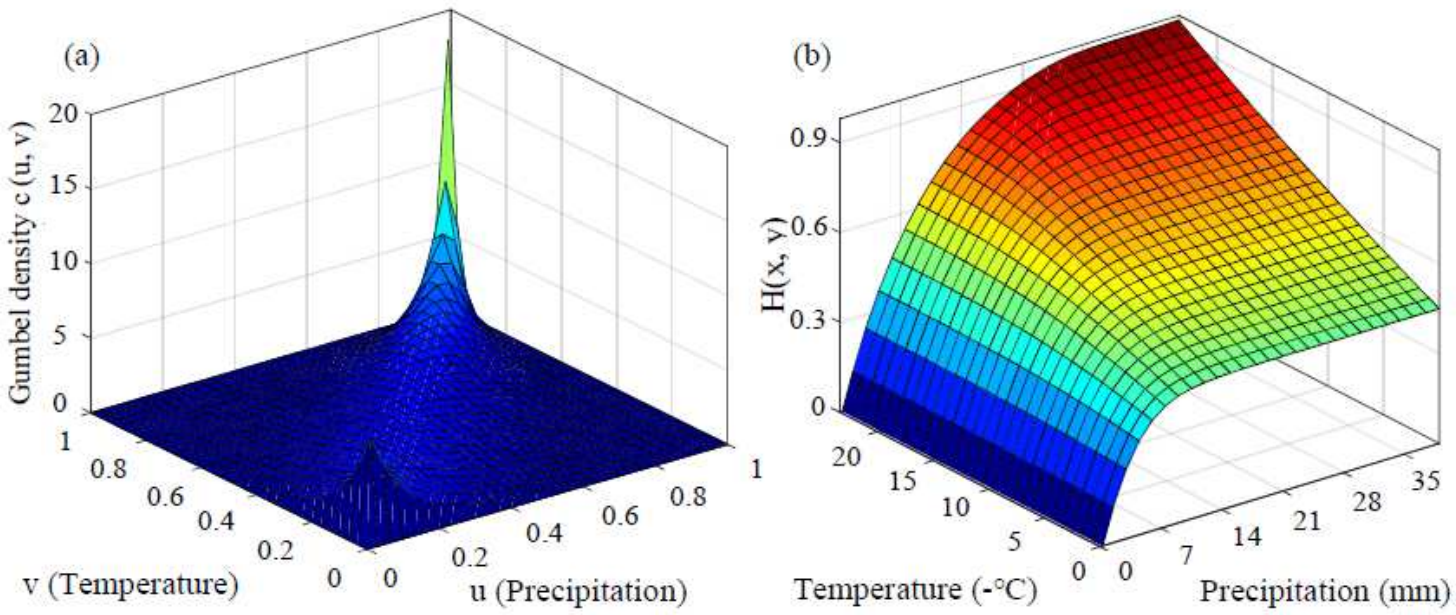

Figure 4

Probability of inducing factors (a) Dependency change; (b) Joint distribution

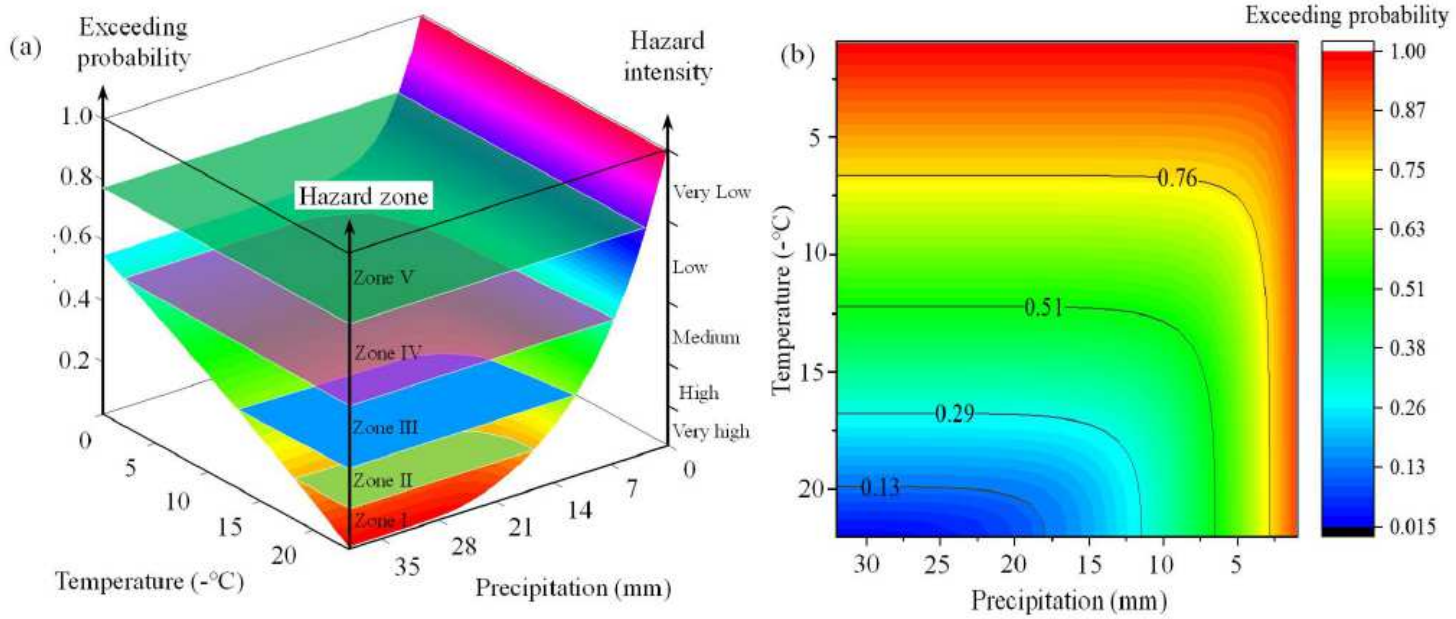

Figure 5

The hazard of icing disaster, (a) Hazard zone, (b) Hazard level

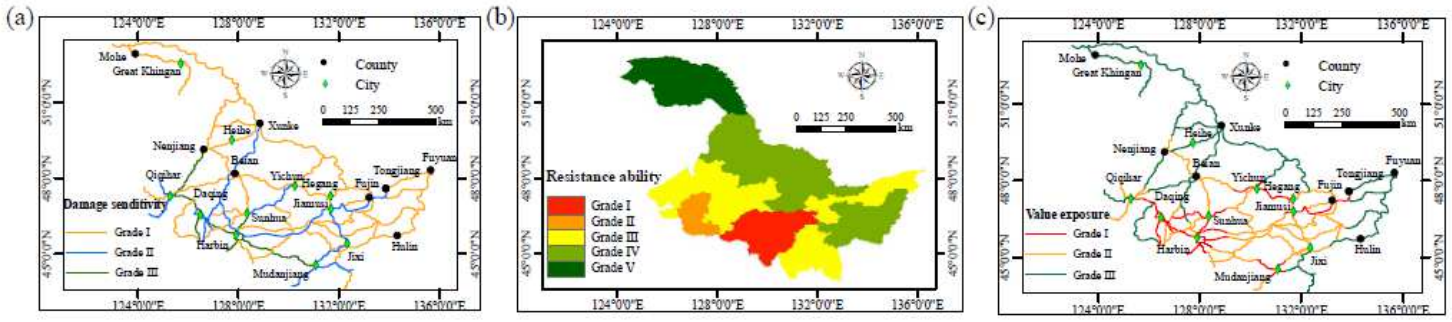

Figure 6

Vulnerability indicators, (a) Damage sensitivity, (b) Economic conditions, 289 (c) Value exposure Note: The designations employed and the presentation of the material on this map do not imply the expression of any opinion whatsoever on the part of Research Square concerning the legal status of any country, territory, city or area or of its authorities, or concerning the delimitation of its frontiers or boundaries. This map has been provided by the authors.

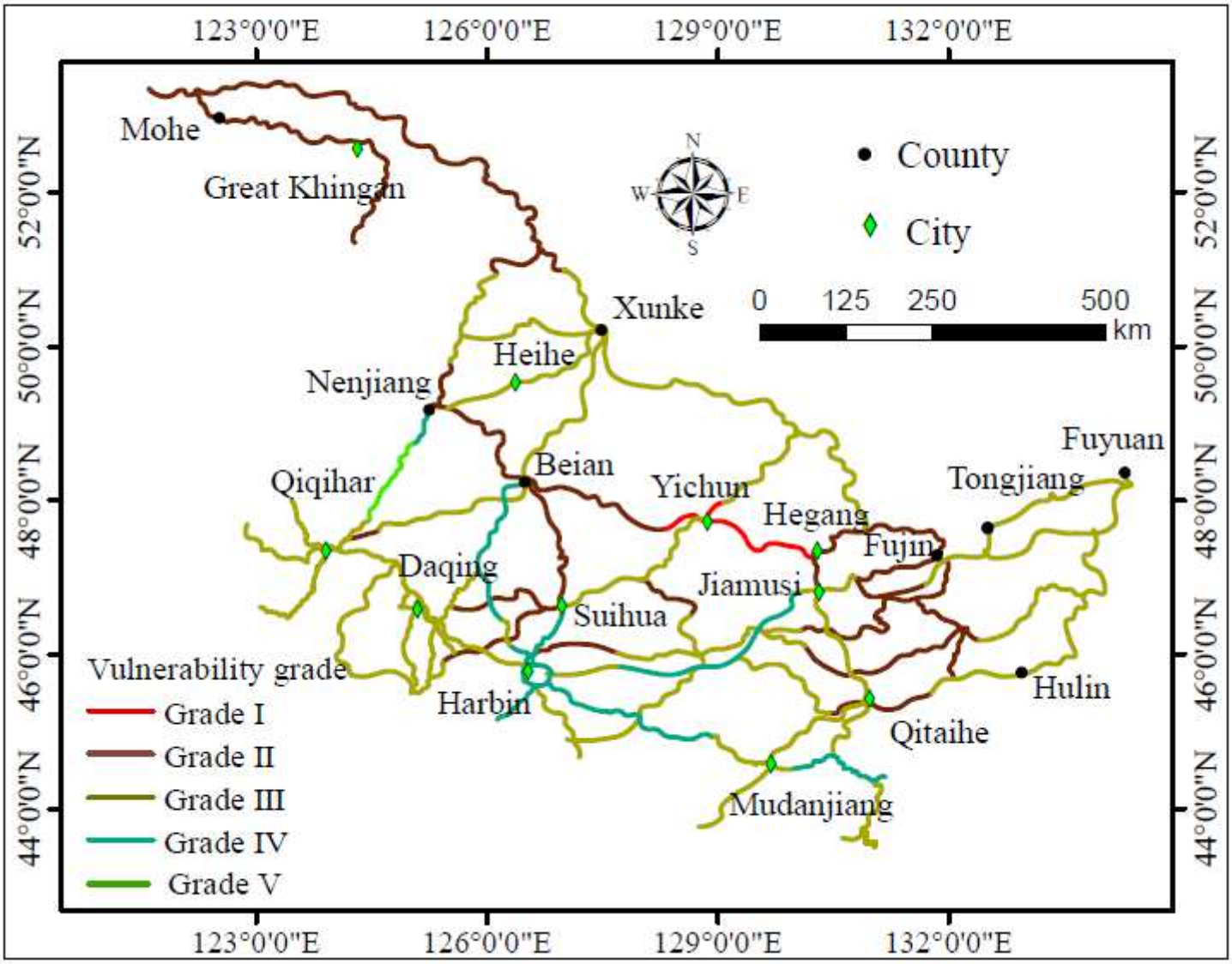

Figure 7

Vulnerability distribution of highways Note: The designations employed and the presentation of the material on this map do not imply the expression of any opinion whatsoever on the part of Research Square concerning the legal status of any country, territory, city or area or of its authorities, or concerning the delimitation of its frontiers or boundaries. This map has been provided by the authors.

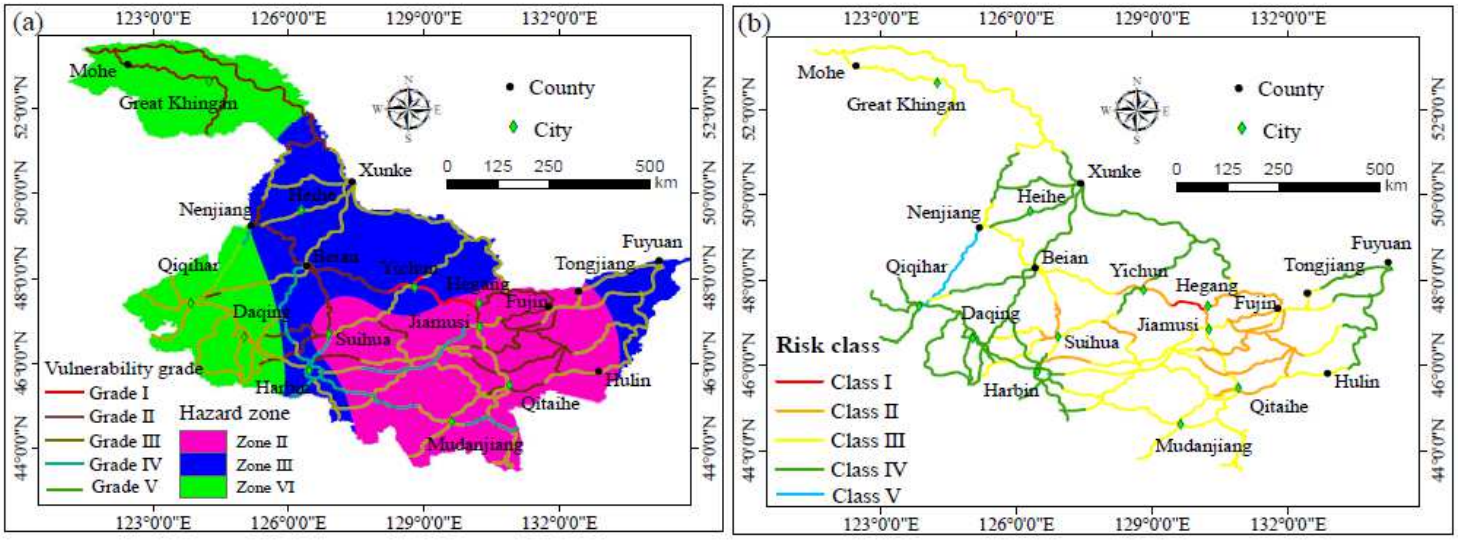

Figure 8

Highway icing analysis, (a) Spatial overlap of hazard and vulnerability, (b) Highway risk distribution Note: The designations employed and the presentation of the material on this map do not imply the expression of any opinion whatsoever on the part of Research Square concerning the legal status of any country, territory, city or area or of its authorities, or concerning the delimitation of its frontiers or boundaries. This map has been provided by the authors.